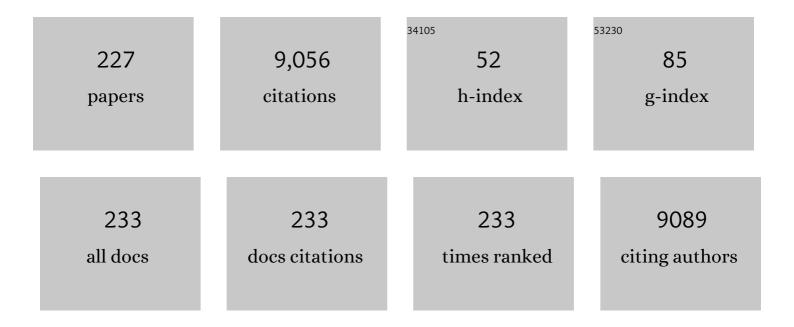
List of Publications by Year in descending order

Source: https://exaly.com/author-pdf/9038668/publications.pdf Version: 2024-02-01



DUNAVELLI

#	Article	IF	CITATIONS
1	Organic and hybrid resistive switching materials and devices. Chemical Society Reviews, 2019, 48, 1531-1565.	38.1	291
2	An Oxide Schottky Junction Artificial Optoelectronic Synapse. ACS Nano, 2019, 13, 2634-2642.	14.6	237
3	Nonvolatile resistive switching in graphene oxide thin films. Applied Physics Letters, 2009, 95, .	3.3	228
4	Observation of Conductance Quantization in Oxideâ€Based Resistive Switching Memory. Advanced Materials, 2012, 24, 3941-3946.	21.0	217
5	Polymer memristor for information storage and neuromorphic applications. Materials Horizons, 2014, 1, 489.	12.2	209
6	A skin-inspired tactile sensor for smart prosthetics. Science Robotics, 2018, 3, .	17.6	195
7	Organic Biomimicking Memristor for Information Storage and Processing Applications. Advanced Electronic Materials, 2016, 2, 1500298.	5.1	181
8	An Optoelectronic Resistive Switching Memory with Integrated Demodulating and Arithmetic Functions. Advanced Materials, 2015, 27, 2797-2803.	21.0	174
9	Light-Gated Memristor with Integrated Logic and Memory Functions. ACS Nano, 2017, 11, 11298-11305.	14.6	173
10	Pushing Extended <i>p</i> -Quinodimethanes to the Limit: Stable Tetracyano-oligo(<i>N</i> -annulated) Tj ETQq 2013, 135, 6363-6371.	0 0 0 rgBT 13.7	/Overlock 10 170
11	Dibenzoheptazethrene Isomers with Different Biradical Characters: An Exercise of Clar's Aromatic Sextet Rule in Singlet Biradicaloids. Journal of the American Chemical Society, 2013, 135, 18229-18236.	13.7	167
12	Thermally Stable Transparent Resistive Random Access Memory based on Allâ€Oxide Heterostructures. Advanced Functional Materials, 2014, 24, 2171-2179.	14.9	150
13	Waterproof, Highly Tough, and Fast Self-Healing Polyurethane for Durable Electronic Skin. ACS Applied Materials & Interfaces, 2020, 12, 11072-11083.	8.0	149
14	Mechanism of nonvolatile resistive switching in graphene oxide thin films. Carbon, 2011, 49, 3796-3802.	10.3	141
15	Phase Manipulating toward Molybdenum Disulfide for Optimizing Electromagnetic Wave Absorbing in Gigahertz. Advanced Functional Materials, 2021, 31, 2011229.	14.9	141
16	Resistance switching in polycrystalline BiFeO3 thin films. Applied Physics Letters, 2010, 97, .	3.3	139
17	Effect of top electrodes on photovoltaic properties of polycrystalline BiFeO ₃ based thin film capacitors. Nanotechnology, 2011, 22, 195201.	2.6	136
18	A Multilevel Memory Based on Proton-Doped Polyazomethine with an Excellent Uniformity in Resistive Switching. Journal of the American Chemical Society, 2012, 134, 17408-17411.	13.7	136

#	Article	IF	CITATIONS
19	Nonvolatile resistive switching memory based on amorphous carbon. Applied Physics Letters, 2010, 96,	3.3	133
20	Metalâ€Organic Framework Nanofilm for Mechanically Flexible Information Storage Applications. Advanced Functional Materials, 2015, 25, 2677-2685.	14.9	133
21	Ultrathin MoS ₂ Nanosheets Encapsulated in Hollow Carbon Spheres: A Case of a Dielectric Absorber with Optimized Impedance for Efficient Microwave Absorption. ACS Applied Materials & Interfaces, 2020, 12, 20785-20796.	8.0	120
22	Mechanism for resistive switching in an oxide-based electrochemical metallization memory. Applied Physics Letters, 2012, 100, .	3.3	117
23	Highly flexible resistive switching memory based on amorphous-nanocrystalline hafnium oxide films. Nanoscale, 2017, 9, 7037-7046.	5.6	109
24	0D/1D/2D architectural Co@C/MXene composite for boosting microwave attenuation performance in 2–18ÂGHz. Carbon, 2022, 193, 182-194.	10.3	108
25	Improvement of resistive switching in Cu/ZnO/Pt sandwiches by weakening the randomicity of the formation/rupture of Cu filaments. Nanotechnology, 2011, 22, 275204.	2.6	106
26	Fe-based amorphous alloys for wide ribbon production with high Bs and outstanding amorphous forming ability. Journal of Alloys and Compounds, 2015, 630, 209-213.	5.5	106
27	Nonvolatile resistive switching in metal/La-doped BiFeO ₃ /Pt sandwiches. Nanotechnology, 2010, 21, 425202.	2.6	104
28	A Resistance-Switchable and Ferroelectric Metal–Organic Framework. Journal of the American Chemical Society, 2014, 136, 17477-17483.	13.7	103
29	Redox gated polymer memristive processing memory unit. Nature Communications, 2019, 10, 736.	12.8	99
30	Mechanically tunable magnetic properties of Fe81Ga19 films grown on flexible substrates. Applied Physics Letters, 2012, 100, .	3.3	93
31	Push–Pull Type Oligo(<i>N</i> -annulated perylene)quinodimethanes: Chain Length and Solvent-Dependent Ground States and Physical Properties. Journal of the American Chemical Society, 2015, 137, 8572-8583.	13.7	93
32	Fast decolorization of azo dyes in both alkaline and acidic solutions by Al-based metallic glasses. Journal of Alloys and Compounds, 2017, 701, 759-767.	5.5	92
33	Printable Liquidâ€Metal@PDMS Stretchable Heater with High Stretchability and Dynamic Stability for Wearable Thermotherapy. Advanced Materials Technologies, 2019, 4, 1800435.	5.8	92
34	The magnetocaloric effect of Gd-Tb-Dy-Al-M (MÂ=ÂFe, Co and Ni) high-entropy bulk metallic glasses. Intermetallics, 2015, 58, 31-35.	3.9	84
35	A 1D Vanadium Dioxide Nanochannel Constructed via Electricâ€Fieldâ€Induced Ion Transport and its Superior Metal–Insulator Transition. Advanced Materials, 2017, 29, 1702162.	21.0	79
36	Hydrogen Bonding in Self-Healing Elastomers. ACS Omega, 2021, 6, 9319-9333.	3.5	79

#	Article	IF	CITATIONS
37	Piezocapacitive Flexible Eâ€Skin Pressure Sensors Having Magnetically Grown Microstructures. Advanced Materials Technologies, 2020, 5, 1900934.	5.8	78
38	Anomalously large anisotropic magnetoresistance in a perovskite manganite. Proceedings of the National Academy of Sciences of the United States of America, 2009, 106, 14224-14229.	7.1	74
39	Correlation between soft-magnetic properties and Tx1-Tc in high Bs FeCoSiBPC amorphous alloys. Journal of Alloys and Compounds, 2016, 659, 193-197.	5.5	72
40	Convertible resistive switching characteristics between memory switching and threshold switching in a single ferritin-based memristor. Chemical Communications, 2016, 52, 4828-4831.	4.1	71
41	Nonvolatile bistable resistive switching in a new polyimide bearing 9-phenyl-9H-carbazole pendant. Journal of Materials Chemistry, 2012, 22, 520-526.	6.7	70
42	Thermally-stable resistive switching with a large ON/OFF ratio achieved in poly(triphenylamine). Chemical Communications, 2014, 50, 11856-11858.	4.1	69
43	Resistive switching effects in oxide sandwiched structures. Frontiers of Materials Science, 2012, 6, 183-206.	2.2	68
44	Improving Unipolar Resistive Switching Uniformity with Cone-Shaped Conducting Filaments and Its Logic-In-Memory Application. ACS Applied Materials & Interfaces, 2018, 10, 6453-6462.	8.0	68
45	Dumbbell-Like Fe ₃ O ₄ @N-Doped Carbon@2H/1T-MoS ₂ with Tailored Magnetic and Dielectric Loss for Efficient Microwave Absorbing. ACS Applied Materials & Interfaces, 2021, 13, 47061-47071.	8.0	62
46	Synaptic plasticity and learning behaviours in flexible artificial synapse based on polymer/viologen system. Journal of Materials Chemistry C, 2016, 4, 3217-3223.	5.5	61
47	Magneto-mechanical coupling effect in amorphous Co40Fe40B20 films grown on flexible substrates. Applied Physics Letters, 2014, 105, .	3.3	60
48	Nanoscale Magnetization Reversal Caused by Electric Field-Induced Ion Migration and Redistribution in Cobalt Ferrite Thin Films. ACS Nano, 2015, 9, 4210-4218.	14.6	60
49	Tunable photovoltaic effects in transparent Pb(Zr0.53,Ti0.47)O3 capacitors. Applied Physics Letters, 2012, 100, .	3.3	58
50	Stretchable Spin Valve with Stable Magnetic Field Sensitivity by Ribbon-Patterned Periodic Wrinkles. ACS Nano, 2016, 10, 4403-4409.	14.6	57
51	Mechano-regulated metal–organic framework nanofilm for ultrasensitive and anti-jamming strain sensing. Nature Communications, 2018, 9, 3813.	12.8	57
52	A Composite Elastic Conductor with High Dynamic Stability Based on 3D alabash Bunch Conductive Network Structure for Wearable Devices. Advanced Electronic Materials, 2018, 4, 1800137.	5.1	57
53	Role of oxadiazole moiety in different D–A polyazothines and related resistive switching properties. Journal of Materials Chemistry C, 2013, 1, 4556.	5.5	56
54	Microstructure dependence of leakage and resistive switching behaviours in Ce-doped BiFeO ₃ thin films. Journal Physics D: Applied Physics, 2011, 44, 415104.	2.8	53

#	Article	IF	CITATIONS
55	Intrinsically Stretchable Resistive Switching Memory Enabled by Combining a Liquid Metal–Based Soft Electrode and a Metal–Organic Framework Insulator. Advanced Electronic Materials, 2019, 5, 1800655.	5.1	53
56	Static and high frequency magnetic properties of FeGa thin films deposited on convex flexible substrates. Applied Physics Letters, 2015, 106, .	3.3	52
57	In Situ Nanoscale Electric Field Control of Magnetism by Nanoionics. Advanced Materials, 2016, 28, 7658-7665.	21.0	52
58	Intrinsic and interfacial effect of electrode metals on the resistive switching behaviors of zinc oxide films. Nanotechnology, 2014, 25, 425204.	2.6	49
59	An organic terpyridyl-iron polymer based memristor for synaptic plasticity and learning behavior simulation. RSC Advances, 2016, 6, 25179-25184.	3.6	48
60	Fabrication of FeSiBPNb amorphous powder cores with high DC-bias and excellent soft magnetic properties. Journal of Magnetism and Magnetic Materials, 2016, 401, 432-435.	2.3	48
61	Amorphous microwires of high entropy alloys with large magnetocaloric effect. Intermetallics, 2018, 96, 79-83.	3.9	48
62	Ultraâ€robust stretchable electrode for eâ€skin: In situ assembly using a nanofiber scaffold and liquid metal to mimic waterâ€toâ€net interaction. InformaÄnÃ-MateriĂ¡ly, 2022, 4, .	17.3	47
63	<i>para</i> â€Quinodimethaneâ€Bridged Perylene Dimers and Pericondensed Quaterrylenes: The Effect of the Fusion Mode on the Ground States and Physical Properties. Chemistry - A European Journal, 2014, 20, 11410-11420.	3.3	46
64	Superparamagnetism and transport properties of ultrafine La2/3Ca1/3MnO3powders. Journal of Physics Condensed Matter, 2001, 13, 141-148.	1.8	45
65	Recent Advances of Quantum Conductance in Memristors. Advanced Electronic Materials, 2019, 5, 1800854.	5.1	44
66	Structural effect on the resistive switching behavior of triphenylamine-based poly(azomethine)s. Chemical Communications, 2014, 50, 11496-11499.	4.1	42
67	Magnetoresistance of La0.5Sr0.5MnO3 nanoparticle compact. Journal of Applied Physics, 2000, 87, 5582-5584.	2.5	39
68	Controllable strain-induced uniaxial anisotropy of Fe81Ga19 films deposited on flexible bowed-substrates. Journal of Applied Physics, 2013, 114, .	2.5	39
69	Anomalous Hall magnetoresistance in a ferromagnet. Nature Communications, 2018, 9, 2255.	12.8	39
70	Magnetic properties and colossal magnetoresistance of the perovskites La2/3Ca1/3Mn1â^'xTixO3. Journal of Applied Physics, 2000, 87, 5597-5599.	2.5	38
71	Magnetic field induced polarization and magnetoelectric effect of Ba0.8Ca0.2TiO3-Ni0.2Cu0.3Zn0.5Fe2O4 nanomultiferroic. Journal of Applied Physics, 2013, 113, .	2.5	37
72	Asymmetric Structure Based Flexible Strain Sensor for Simultaneous Detection of Various Human Joint Motions. ACS Applied Electronic Materials, 2019, 1, 1866-1872.	4.3	35

#	Article	IF	CITATIONS
73	Positive temperature coefficient of magnetic anisotropy in polyvinylidene fluoride (PVDF)-based magnetic composites. Scientific Reports, 2014, 4, 6615.	3.3	34
74	Effect of buffer layer and external stress on magnetic properties of flexible FeGa films. Journal of Applied Physics, 2013, 113, .	2.5	33
75	Recovery of gold from hydrometallurgical leaching solution of electronic waste via spontaneous reduction by polyaniline. Progress in Natural Science: Materials International, 2017, 27, 514-519.	4.4	33
76	Liquid Metalâ€Based Strain Sensor with Ultralow Detection Limit for Human–Machine Interface Applications. Advanced Intelligent Systems, 2021, 3, 2000235.	6.1	33
77	Electromagnetic and microwave-absorbing properties of Co-based amorphous wire and Ce2Fe17N3-δ composite. Journal of Alloys and Compounds, 2018, 730, 255-260.	5.5	32
78	Recyclable Liquid Metalâ€Based Circuit on Paper. Advanced Materials Technologies, 2018, 3, 1800131.	5.8	32
79	Nanoscale observation of room-temperature ferromagnetism on ultrathin (La,Ba)MnO3 films. Applied Physics Letters, 2003, 83, 1184-1186.	3.3	31
80	Fieldlike spin-orbit torque in ultrathin polycrystalline FeMn films. Physical Review B, 2016, 93, .	3.2	31
81	Controllable and Stable Quantized Conductance States in a Pt/HfO <i>_x</i> /ITO Memristor. Advanced Electronic Materials, 2020, 6, 1901055.	5.1	31
82	Synthesis of single-crystal La0.67Sr0.33MnO3 freestanding films with different crystal-orientation. APL Materials, 2020, 8, .	5.1	31
83	Synthesis and nonvolatile memristive switching effect of a donor–acceptor structured oligomer. Journal of Materials Chemistry C, 2015, 3, 664-673.	5.5	29
84	Magnetic softness and magnetization dynamics of FeSiBNbCu(P,Mo) nanocrystalline alloys with good high-frequency characterization. Journal of Magnetism and Magnetic Materials, 2019, 478, 192-197.	2.3	29
85	A Wearable Capacitive Sensor Based on Ring/Disk‣haped Electrode and Porous Dielectric for Noncontact Healthcare Monitoring. Global Challenges, 2020, 4, 1900079.	3.6	29
86	Microwave absorption properties of planar-anisotropy Ce 2 Fe 17 N 3 â~δ powders/Silicone composite in X-band. Journal of Magnetism and Magnetic Materials, 2017, 424, 39-43.	2.3	28
87	Magnetocaloric effect in Fe–Tm–B–Nb metallic glasses near room temperature. Journal of Non-Crystalline Solids, 2015, 425, 114-117.	3.1	27
88	Microwave absorbing properties of FeCrMoNiPBCSi amorphous powders composite. Journal of Alloys and Compounds, 2017, 705, 309-313.	5.5	27
89	Self-powered stretchable strain sensors for motion monitoring and wireless control. Nano Energy, 2022, 92, 106754.	16.0	27
90	Surface morphology and magnetic property of wrinkled FeGa thin films fabricated on elastic polydimethylsiloxane. Applied Physics Letters, 2016, 108, .	3.3	26

#	Article	IF	CITATIONS
91	Flexible supercapacitor electrodes fabricated by dealloying nanocrystallized Al-Ni-Co-Y-Cu metallic glasses. Journal of Alloys and Compounds, 2019, 772, 164-172.	5.5	26
92	Pure spin-Hall magnetoresistance in Rh/Y3Fe5O12 hybrid. Scientific Reports, 2015, 5, 17734.	3.3	25
93	Controlled Construction of Atomic Point Contact with 16 Quantized Conductance States in Oxide Resistive Switching Memory. ACS Applied Electronic Materials, 2019, 1, 789-798.	4.3	25
94	Nanopatterning of perovskite manganite thin films by atomic force microscope lithography. Nanotechnology, 2005, 16, 28-31.	2.6	24
95	Effect of epitaxial strain and lattice mismatch on magnetic and transport behaviors in metamagnetic FeRh thin films. AIP Advances, 2017, 7, .	1.3	24
96	Composition Effect on Intrinsic Plasticity or Brittleness in Metallic Glasses. Scientific Reports, 2014, 4, 5733.	3.3	23
97	Magnetic anisotropy and high-frequency property of flexible FeCoTa films obliquely deposited on a wrinkled topography. Scientific Reports, 2017, 7, 2837.	3.3	23
98	Atomic force microscope lithography in perovskite manganite La0.8Ba0.2MnO3 films. Journal of Applied Physics, 2004, 95, 7091-7093.	2.5	22
99	Evolution of shear bands into cracks in metallic glasses. Journal of Alloys and Compounds, 2015, 621, 238-243.	5.5	22
100	Magnetostrictive GMR spin valves with composite FeGa/FeCo free layers. AIP Advances, 2016, 6, .	1.3	22
101	Enhanced stress-invariance of magnetization direction in magnetic thin films. Applied Physics Letters, 2017, 111, .	3.3	22
102	Preparation and ferroelectric properties of freestanding Pb(Zr,Ti)O ₃ thin membranes. Journal Physics D: Applied Physics, 2012, 45, 185302.	2.8	21
103	Resistance-Switchable Graphene Oxide-Polymer Nanocomposites for Molecular Electronics. ChemElectroChem, 2014, 1, 514-519.	3.4	21
104	Tuning magnetic anisotropy of amorphous CoFeB film by depositing on convex flexible substrates. AIP Advances, 2016, 6, .	1.3	21
105	Nanoporous metal/metal-oxide composite prepared by one-step de-alloying AlNiCoYCu metallic glasses. Journal of Alloys and Compounds, 2017, 703, 461-465.	5.5	21
106	Rapid detection of Escherichia coli O157:H7 using tunneling magnetoresistance biosensor. AIP Advances, 2017, 7, .	1.3	21
107	Cooperative control of perpendicular magnetic anisotropy via crystal structure and orientation in freestanding SrRuO3 membranes. Npj Flexible Electronics, 2022, 6, .	10.7	21
108	Tunneling magnetoresistance induced by controllable formation of Co filaments in resistive switching Co/ZnO/Fe structures. Europhysics Letters, 2014, 108, 58004.	2.0	20

#	Article	IF	CITATIONS
109	Thin and broadband Ce2Fe17N3-Î/MWCNTs composite absorber with efficient microwave absorption. Journal of Alloys and Compounds, 2019, 787, 1097-1103.	5.5	20
110	Stretchable tactile sensor with high sensitivity and dynamic stability based on vertically aligned urchin-shaped nanoparticles. Materials Today Physics, 2020, 14, 100219.	6.0	20
111	Large low-field magnetoresistance of phase-separated single-crystalline Pr0.7Pb0.3MnO3. Applied Physics Letters, 2002, 80, 3367-3369.	3.3	19
112	Magnetization reversal in epitaxial exchange-biased IrMn/FeGa bilayers with anisotropy geometries controlled by oblique deposition. Physical Review B, 2015, 91, .	3.2	19
113	Flexural Strength and Weibull Analysis of Bulk Metallic Glasses. Journal of Materials Science and Technology, 2016, 32, 129-133.	10.7	19
114	Development of FeNiNbSiBP bulk metallic glassy alloys with excellent magnetic properties and high glass forming ability evaluated by different criterions. Intermetallics, 2016, 71, 1-6.	3.9	19
115	Determination of stress-coefficient of magnetoelastic anisotropy in flexible amorphous CoFeB film by anisotropic magnetoresistance. Applied Physics Letters, 2017, 111, .	3.3	19
116	Thickness-dependent and strain-tunable magnetism in two-dimensional van der Waals VSe2. Nano Research, 2022, 15, 7597-7603.	10.4	19
117	Antiferro- to ferromagnetic transition and large magnetoresistance in YMn6Sn6â^'xTix (x=0–1.0) compounds. Journal of Applied Physics, 2002, 91, 5250-5253.	2.5	18
118	Giant anisotropic magnetoresistance in bilayered La1.2Sr1.8Mn2O7 single crystals. Applied Physics Letters, 2011, 98, 212503.	3.3	18
119	The evolution of relaxation modes during isothermal annealing and its influence on properties of Fe-based metallic glass. Journal of Non-Crystalline Solids, 2019, 509, 95-98.	3.1	18
120	Magnetocrystalline anisotropy imprinting of an antiferromagnet on an amorphous ferromagnet in FeRh/CoFeB heterostructures. NPG Asia Materials, 2020, 12, .	7.9	18
121	Anisotropic magnetoresistance in polycrystalline La _{0.67} (Ca _{1â^x} Sr _x) _{0.33} MnO ₃ . Journal Physics D: Applied Physics, 2012, 45, 245001.	2.8	17
122	In-plane anisotropic converse magnetoelectric coupling effect in FeGa/polyvinylidene fluoride heterostructure films. Journal of Applied Physics, 2013, 113, .	2.5	17
123	Bioâ€Inspired Multiâ€Mode Painâ€Perceptual System (MMPPS) with Noxious Stimuli Warning, Damage Localization, and Enhanced Damage Protection. Advanced Science, 2021, 8, 2004208.	11.2	17
124	An Antifatigue Liquid Metal Composite Electrode Ionic Polymer-Metal Composite Artificial Muscle with Excellent Electromechanical Properties. ACS Applied Materials & Interfaces, 2022, 14, 14630-14639.	8.0	17
125	Magnetocaloric effect of Fe–RE–B–Nb (RE = Tb, Ho or Tm) bulk metallic glasses with high glass-forming ability. Journal of Alloys and Compounds, 2015, 644, 346-349.	5.5	16
126	Manipulation of Exchange Bias Effect via All-Solid-State <mml:math xmlns:mml="http://www.w3.org/1998/Math/MathML" display="inline" overflow="scroll"><mml:mi>Li</mml:mi> -Ion Redox Capacitor with Antiferromagnetic Electrode. Physical Review Applied, 2020, 14, .</mml:math 	3.8	16

#	Article	IF	CITATIONS
127	Relaxation of nanopatterns on Nb-doped SrTiO3 surface. Applied Physics Letters, 2004, 84, 2670-2672.	3.3	15
128	Implementation of All 27 Possible Univariate Ternary Logics With a Single ZnO Memristor. IEEE Transactions on Electron Devices, 2019, 66, 4710-4715.	3.0	15
129	Ten States of Nonvolatile Memory through Engineering Ferromagnetic Remanent Magnetization. Advanced Functional Materials, 2019, 29, 1806460.	14.9	15
130	Emergent Ferroelectricity in Otherwise Nonferroelectric Oxides by Oxygen Vacancy Design at Heterointerfaces. ACS Applied Materials & Interfaces, 2020, 12, 45602-45610.	8.0	15
131	Colossal angular magnetoresistance in the antiferromagnetic semiconductor <mml:math xmlns:mml="http://www.w3.org/1998/Math/MathML"><mml:msub><mml:mi>EuTe</mml:mi><mml:mn>2Physical Review B, 2021, 104, .</mml:mn></mml:msub></mml:math 	:m a. 2 <td>ոլ։ութորթուն</td>	ո լ։ու թորթուն
132	Electric-field control of magnetic anisotropy in Fe81Ga19/BaTiO3 heterostructure films. AIP Advances, 2014, 4, 117113.	1.3	14
133	Extraordinary Hall resistance and unconventional magnetoresistance in <mml:math xmlns:mml="http://www.w3.org/1998/Math/MathML"><mml:msub><mml:mrow><mml:mi>Pt</mml:mi><mml:m Physical Review B, 2015, 92, .</mml:m </mml:mrow></mml:msub></mml:math 	o <i>\$.2</i> /mml:	.m ⊅ • < mml:m
134	Structure and magnetic properties of (x= 0-3) compounds with R = Y and Pr. Journal of Physics Condensed Matter, 1998, 10, 2445-2452.	1.8	13
135	Dynamic magnetic characteristics of Fe78Si13B9 amorphous alloy subjected to operating temperature. Journal of Magnetism and Magnetic Materials, 2016, 408, 159-163.	2.3	13
136	Materials with strong spin-textured bands. Npj Quantum Materials, 2020, 5, .	5.2	13
137	Emergent ferromagnetism with tunable perpendicular magnetic anisotropy in short-periodic SrIrO3/SrRuO3 superlattices. Applied Physics Letters, 2020, 116, .	3.3	13
138	A flexible dual-gate hetero-synaptic transistor for spatiotemporal information processing. Nanoscale Advances, 2022, 4, 2412-2419.	4.6	13
139	Thermally assisted electric field control of magnetism in flexible multiferroic heterostructures. Scientific Reports, 2015, 4, 6925.	3.3	12
140	2D Magnetic Mesocrystals for Bit Patterned Media. Advanced Materials Interfaces, 2018, 5, 1800997.	3.7	12
141	Magnetoelastic anisotropy of antiferromagnetic materials. Applied Physics Letters, 2019, 115, .	3.3	12
142	A Stretchable Capacitive Strain Sensor Having Adjustable Elastic Modulus Capability for Wideâ€Range Force Detection. Advanced Engineering Materials, 2020, 22, 1901239.	3.5	12
143	Oxygen vacancy enhanced ferroelectricity in BTO:SRO nanocomposite films. Acta Materialia, 2020, 199, 9-18.	7.9	12
144	Crystallization Behavior of FeSiBPCu Nanocrystalline Soft-Magnetic Alloys with High Fe Content. Science of Advanced Materials, 2015, 7, 2721-2725.	0.7	12

#	Article	IF	CITATIONS
145	2D Nanovaristors at Grain Boundaries Account for Memristive Switching in Polycrystalline BiFeO ₃ . Advanced Electronic Materials, 2015, 1, 1500019.	5.1	11
146	Interactions of Shear Bands in a Ductile Metallic Glass. Journal of Iron and Steel Research International, 2016, 23, 48-52.	2.8	11
147	Direct imaging of cross-sectional magnetization reversal in an exchange-biased CoFeB/IrMn bilayer. Physical Review B, 2018, 97, .	3.2	11
148	Industrialization of a FeSiBNbCu nanocrystalline alloy with high Bs of 1.39ÂT and outstanding soft magnetic properties. Journal of Materials Science: Materials in Electronics, 2018, 29, 19517-19523.	2.2	11
149	Reversibly controlled magnetic domains of Co film via electric field driven oxygen migration at nanoscale. Applied Physics Letters, 2019, 114, . Reversible Control of Magnetic Anisotropy and Magnetization in Amorphous <mml:math< td=""><td>3.3</td><td>11</td></mml:math<>	3.3	11
150	xmlns:mml="http://www.w3.org/1998/Math/MathML" display="inline" overflow="scroll"> <mml:msub><mml:mi>Co</mml:mi><mml:mn>40</mml:mn></mml:msub> <mml:msub><mr mathvariant="normal">B<mml:mn>20</mml:mn></mr </mml:msub> Thin Films via All-Solid-State <mml:math displ.<="" td="" xmlns:mml="http://www.w3.org/1998/Math/MathML"><td>nl:mj>Fe<!--<br-->ath></td><td>mml:mi><mm 11</mm </td></mml:math>	nl:mj>Fe <br ath>	mml:mi> <mm 11</mm
151	Physical Review Applied, 2019, 12 Anti-oxidative passivation and electrochemical activation of black phosphorus <i>via</i> covalent functionalization and its nonvolatile memory application. Journal of Materials Chemistry C, 2020, 8, 7309-7313.	5.5	11
152	Effects of Si content on structure and soft magnetic properties of Fe81.3SixB17-xCu1.7 nanocrystalline alloys with pre-existing α-Fe nanocrystals. Journal of Materials Science, 2021, 56, 2539-2548.	3.7	11
153	Liquid Metal Based Nano-Composites for Printable Stretchable Electronics. Sensors, 2022, 22, 2516.	3.8	11
154	Magnetic glass behavior and magnetoresistive properties of perovskite cobaltitesLa0.7Sr0.3Co1â~'yGayO3. Physical Review B, 1999, 60, 14541-14544.	3.2	10
155	Low-temperature magnetization step and its training effects in phase-separated La0.5Ca0.5MnO3. Journal of Physics Condensed Matter, 2001, 13, 1973-1978.	1.8	10
156	Magnetic transition and large low-field magnetoresistance near Curie temperature in polycrystalline La2/3A1/3MnO3 (A=Ca,Sr). Journal of Applied Physics, 2003, 93, 8092-8094.	2.5	10
157	Stretchable and Twistable Resistive Switching Memory with Information Storage and Computing Functionalities. Advanced Materials Technologies, 2021, 6, 2000810.	5.8	10
158	Structure, magnetic properties and phase separation of Nd0.5Ca0.5Mn1â^'xGaxO3 (၀ြိုးစိုးလို၀.1). Journal of Magnetism and Magnetic Materials, 2003, 265, 248-256.	2.3	9
159	Strain induced tunable anisotropic magnetoresistance in La0.67Ca0.33MnO3/BaTiO3 heterostructures. Journal of Applied Physics, 2013, 113, 17C716.	2.5	9
160	Ion transport-related resistive switching in film sandwich structures. Science Bulletin, 2014, 59, 2363-2382.	1.7	9
161	Strain assisted electrocaloric effect in PbZr0.95Ti0.05O3 films on 0.7Pb(Mg1/3Nb2/3)O3-0.3PbTiO3 substrate. Scientific Reports, 2015, 5, 16164.	3.3	9
162	High-throughput investigation of orientations effect on nanoscale magnetization reversal in cobalt ferrite thin films induced by electric field. Applied Physics Letters, 2017, 111, 162401.	3.3	9

#	Article	IF	CITATIONS
163	Lattice-Mismatch-Induced Oscillatory Feature Size and Its Impact on the Physical Limitation of Grain Size. Physical Review Applied, 2018, 9, .	3.8	9
164	Method for Assembling Nanosamples and a Cantilever for Dynamic Cantilever Magnetometry. Physical Review Applied, 2019, 11, .	3.8	9
165	A visible light-triggered artificial photonic nociceptor with adaptive tunability of threshold. Nanoscale, 2021, 13, 1029-1037.	5.6	9
166	Direct observation of phase separation in La0.45Sr0.55MnO3â^'Î′. Journal of Applied Physics, 2002, 92, 7404-7407.	2.5	8
167	Thermal stability of Al nanocluster arrays on Si (111)-7 × 7 surfaces. Nanotechnology, 2006, 17, 2018-2022.	2.6	8
168	Possible origins of the magnetoresistance gain in colossal magnetoresistive oxide La0.69Ca0.31MnO3: Structure fluctuation and pinning effect on magnetic domain walls. Applied Physics Letters, 2009, 95, 092504.	3.3	8
169	Preparation of nanoporous silver micro-particles through ultrasonic-assisted dealloying of Mg-Ag alloy ribbons. Materials Letters, 2015, 144, 138-141.	2.6	8
170	Reversible Luminescence Modulation upon an Electric Field on a Full Solid-State Device Based on Lanthanide Dimers. ACS Applied Materials & Interfaces, 2016, 8, 15551-15556.	8.0	8
171	Enhanced and broadband absorber with surface pattern design for X-Band. Current Applied Physics, 2018, 18, 55-60.	2.4	8
172	Strain-Insensitive Elastic Surface Electromyographic (sEMG) Electrode for Efficient Recognition of Exercise Intensities. Micromachines, 2020, 11, 239.	2.9	8
173	Stress-coefficient of magnetoelastic anisotropy in flexible Fe, Co and Ni thin films. Journal of Magnetism and Magnetic Materials, 2020, 505, 166750.	2.3	8
174	A flexible metamaterial based on liquid metal patterns embedded in magnetic medium for lightweight microwave absorber. Materials Research Bulletin, 2021, 137, 111199.	5.2	8
175	Emergence of Insulating Ferrimagnetism and Perpendicular Magnetic Anisotropy in 3d–5d Perovskite Oxide Composite Films for Insulator Spintronics. ACS Applied Materials & Interfaces, 2022, 14, 15407-15414.	8.0	8
176	Anisotropic magnetoresistance in epitaxial La0.67(Ca1â^xSrx)0.33MnO3 films. Journal of Applied Physics, 2013, 113, 17C722.	2.5	7
177	Anisotropic field-induced melting of orbital ordered structure inPr0.6Ca0.4MnO3. Physical Review B, 2015, 91, .	3.2	7
178	Preparation and magnetic properties of (Co0.6Fe0.3Ni0.1)70â^'x (B0.811Si0.189)25+x Nb5 bulk glassy alloys. Journal of Materials Science: Materials in Electronics, 2015, 26, 7006-7012.	2.2	7
179	Fe78Si9B13 amorphous powder core with improved magnetic properties. Journal of Materials Science: Materials in Electronics, 2017, 28, 1180-1185.	2.2	7
180	Nanoscale magnetization reversal by electric field-induced ion migration. MRS Communications, 2019, 9, 14-26.	1.8	7

#	Article	IF	CITATIONS
181	Effect of isothermal crystallization in antiferromagnetic IrMn on the formation of spontaneous exchange bias. Applied Physics Letters, 2021, 118, .	3.3	7
182	Liquid Metalâ€Based Strain Sensor with Ultralow Detection Limit for Human–Machine Interface Applications. Advanced Intelligent Systems, 2021, 3, 2170073.	6.1	7
183	Effects of the relative proportion of ferromagnetic and charge-ordered phases on the metal–insulator transition temperature in La0.5Ca0.5Mn1â^'xGexO3. Journal of Applied Physics, 2000, 88, 7041-7044.	2.5	6
184	Magnetic and transport properties of Sn-doped La0.5Ca0.5MnO3. Journal Physics D: Applied Physics, 2000, 33, 1982-1984.	2.8	6
185	Anomalous anisotropic magnetoresistance effects in graphene. AIP Advances, 2014, 4, 097101.	1.3	6
186	High strength CoFe-based glassy alloy with high thermal stability. Materials Letters, 2014, 114, 126-128.	2.6	6
187	Effect of IrMn inserted layer on anomalous-Hall resistance and spin-Hall magnetoresistance in Pt/IrMn/YIG heterostructures. Journal of Applied Physics, 2016, 120, .	2.5	6
188	A univariate ternary logic and three-valued multiplier implemented in a nano-columnar crystalline zinc oxide memristor. RSC Advances, 2019, 9, 24595-24602.	3.6	6
189	Magnetism modulation and conductance quantization in a gadolinium oxide memristor. Physical Chemistry Chemical Physics, 2020, 22, 26322-26329.	2.8	6
190	A Stretchable Capacitive Strain Sensor Having Adjustable Elastic Modulus Capability for Wideâ€Range Force Detection. Advanced Engineering Materials, 2020, 22, 2070011.	3.5	6
191	Lattice effects of doping the Mn sites in La0.5Ca0.5MnO3. Journal of Applied Physics, 2000, 88, 5924-5927.	2.5	5
192	Magnetoinductance and magnetoimpedance response of Co-based multi-wire arrays. Journal of Magnetism and Magnetic Materials, 2015, 393, 278-283.	2.3	5
193	Lateral Modulation of Magnetic Anisotropy in Tricolor 3d–5d Oxide Superlattices. ACS Applied Electronic Materials, 2021, 3, 4210-4217.	4.3	5
194	Unusual anisotropic magnetoresistance in charge-orbital ordered Nd0.5Sr0.5MnO3 polycrystals. Journal of Applied Physics, 2014, 116, .	2.5	4
195	Influence of Thermal Deformation on Exchange Bias in FeGa/IrMn Bilayers Grown on Flexible Polyvinylidene Fluoride Membranes. IEEE Transactions on Magnetics, 2016, 52, 1-4.	2.1	4
196	Polyaniline-poly(vinylidene fluoride) blend microfiltration membrane and its spontaneous gold recovery application. Science China Chemistry, 2018, 61, 118-126.	8.2	4
197	Multifunctional Optoelectronic Device Based on Resistive Switching Effects. , 0, , .		4
198	A novel approach based on magneto-electric torque sensor for non-contact biomarkers detection. Sensors and Actuators B: Chemical, 2018, 276, 540-544.	7.8	4

#	Article	IF	CITATIONS
199	Spin-valve-like magnetoresistance in a Ni-Mn-In thin film. Physical Review B, 2018, 97, .	3.2	4
200	Inferring the magnetic anisotropy of a nanosample through dynamic cantilever magnetometry measurements. Applied Physics Letters, 2020, 116, 193102.	3.3	4
201	Phase separation induced by doping at Mn sites in Nd[sub 0.5]Ca[sub 0.5]Mn[sub 0.98]Ga[sub 0.02]O[sub 3]. Journal of Applied Physics, 2002, 91, 7941.	2.5	3
202	Magnetism, transport, and specific heat of electronically phase-separated Pr _{0.7} Pb _{0.3} MnO ₃ single crystals. Journal of Physics Condensed Matter, 2009, 21, 076002.	1.8	3
203	Fabrication of FePBNbCr Glassy Cores With Good Soft Magnetic Properties by Hot Pressing. IEEE Transactions on Magnetics, 2015, 51, 1-4.	2.1	3
204	Preparation and magnetic properties of wrinkled FeRh flexible films. AIP Advances, 2020, 10, 025327.	1.3	3
205	Crystal Orientations Dependent Polarization Reversal in Ferroelectric PbZr 0.2 Ti 0.8 O 3 Thin Films for Multilevel Data Storage Applications. Advanced Materials Interfaces, 2021, 8, 2100871.	3.7	3
206	lsostructural metal-insulator transition driven by dimensional-crossover in <mml:math xmlns:mml="http://www.w3.org/1998/Math/MathML"><mml:msub><mml:mi>SrIrO</mml:mi><mml:mn>3heterostructures. Physical Review Materials, 2022, 6, .</mml:mn></mml:msub></mml:math 	ւ∣:m₂n₄ 	ml :ø nsub>
207	Resistive Switching Memories: Observation of Conductance Quantization in Oxideâ€Based Resistive Switching Memory (Adv. Mater. 29/2012). Advanced Materials, 2012, 24, 3898-3898.	21.0	2
208	Transparent Electronics: Thermally Stable Transparent Resistive Random Access Memory based on Allâ€Oxide Heterostructures (Adv. Funct. Mater. 15/2014). Advanced Functional Materials, 2014, 24, 2110-2110.	14.9	2
209	Role of the Co-based microwires/polymer matrix interface on giant magneto impedance response. Journal of Alloys and Compounds, 2015, 643, S95-S98.	5.5	2
210	Magnetic Anisotropy and Reversal in Epitaxial FeGa/MgO(001) Films Deposited at Oblique Incidence. IEEE Transactions on Magnetics, 2015, 51, 1-4.	2.1	2
211	Nonlinear fragile-to-strong transition in a magnetic glass system driven by magnetic field. AIP Advances, 2017, 7, 125014.	1.3	2
212	Quantum Conductance: Recent Advances of Quantum Conductance in Memristors (Adv. Electron.) Tj ETQq0 0 () rg <u>BT</u> /Ov	erlock 10 Tf 5
213	Layer-by-layer epitaxial growth of monoclinic SrIrO3 thin films on (111)-oriented SrTiO3 through interface engineering. Thin Solid Films, 2020, 709, 138119.	1.8	2
214	Ordered Nano-Islands on (La,Ba)MnO ₃ Thin Film Surface by Self-Organization. Journal of Nanoscience and Nanotechnology, 2004, 4, 982-985.	0.9	1
215	Current effects and topology of current paths in single crystalline Pr[sub 0.7]Pb[sub 0.3]MnO[sub 3]. Journal of Applied Physics, 2006, 100, 113902.	2.5	1
216	Nonvolatile Memory: Metalâ€Organic Framework Nanofilm for Mechanically Flexible Information Storage Applications (Adv. Funct. Mater. 18/2015). Advanced Functional Materials, 2015, 25, 2630-2630.	14.9	1

#	Article	IF	CITATIONS
217	Modulation of Magnetic Anisotropy in Flexible Multiferroic FeGa/PVDF Heterostructures Under Various Strains. IEEE Transactions on Magnetics, 2015, 51, 1-4.	2.1	1
218	Functional Oxide Thin Films and Nanostructures: Growth, Interface, and Applications. Journal of Nanomaterials, 2016, 2016, 1-2.	2.7	1
219	Nanochannels: A 1D Vanadium Dioxide Nanochannel Constructed via Electricâ€Fieldâ€Induced Ion Transport and its Superior Metal–Insulator Transition (Adv. Mater. 39/2017). Advanced Materials, 2017, 29, .	21.0	1
220	Electric Field Control of Magnetic Properties by Means of Li+ Migration in FeRh Thin Film. Magnetochemistry, 2021, 7, 45.	2.4	1
221	Mechanical Analysis and Experimental Studies of the Transverse Strain in Wrinkled Metallic Thin Films. Metals, 2021, 11, 427.	2.3	1
222	Multiâ€Mode Painâ€Perceptual System: Bioâ€Inspired Multiâ€Mode Painâ€Perceptual System (MMPPS) with Noxious Stimuli Warning, Damage Localization, and Enhanced Damage Protection (Adv. Sci. 10/2021). Advanced Science, 2021, 8, 2170055.	11.2	1
223	Initial Adsorption of C60 Molecules on Si(111)-7*7 Surface with Al Nanocluster Array. E-Journal of Surface Science and Nanotechnology, 2010, 8, 354-357.	0.4	1
224	Magnetocrystalline anisotropy of Y2(Fe1-xCox)15Ga2compounds. Journal Physics D: Applied Physics, 2000, 33, 1446-1449.	2.8	0
225	Switching Memory: An Optoelectronic Resistive Switching Memory with Integrated Demodulating and Arithmetic Functions (Adv. Mater. 17/2015). Advanced Materials, 2015, 27, 2812-2812.	21.0	0
226	Elastic Conductors: A Composite Elastic Conductor with High Dynamic Stability Based on 3D-Calabash Bunch Conductive Network Structure for Wearable Devices (Adv. Electron. Mater. 9/2018). Advanced Electronic Materials, 2018, 4, 1870045.	5.1	0
227	Observation of Atomicâ€Order Engineered Martensitic Transformation in Ni 45 Co 5 Mn 37 In 13 Metamagnetic Shape Memory Alloys. Advanced Engineering Materials, 0, , 2100711.	3.5	Ο